Long-Duration Observation of Propagating Slow Magnetoacoustic Waves

Ding Yuan, Valery Nakariakov and Claire Foullon

CFSA, Department of Physics, University of Warwick, Coventry, CV4 7AL

Introduction

Propagating intensity perturbations are observed confidently in EUV bandpasses along polar plumes and coronal loops with modern instruments, e.g, SOHO/EIT, TRACE and recently with Hinode/EIT and XRT. The intensity perturbations are found to travel at projected speeds lower than the local sound speed due to projection effects and was interpreted as slow-mode magneto-acoustic waves (e.g. Nakariakov & Verwichte 2005, De Moortel 2006). According to De Moortel (2009), the propagating perturbations usually have small variations ($\sim 4\%$) of the background intensity, they are often found in form of wave trains in large quiescent loops near the edge of active regions, oscillating at periods of ~ 3 mins above sunspot umbras and ~ 5 mins off sunspots (above plage region). The waves are observed to last for at least several hours, while their parameters (the speed, and amplitude, period) do not seem to vary in time, while there has not been any dedicated study of the long-term variability.

Motivation

The main objective of our work is to investigate the evolutionary features of the slow-mode magneto-acoustic waves over long-duration (several days), in two EUV bandpasses (TRACE 171 Å and 195 Å), focusing on:

- Propagating speed variation
- Frequency changes
- Phase stability

Data set

Long-term observation (30 June to 4 July 1998) was performed by TRACE over active region AR8253 at full spatial resolution (0.5 arcsec/pixel) over half FOV 512×512 pixels in two EUV bandpasses (171Å and 195Å).

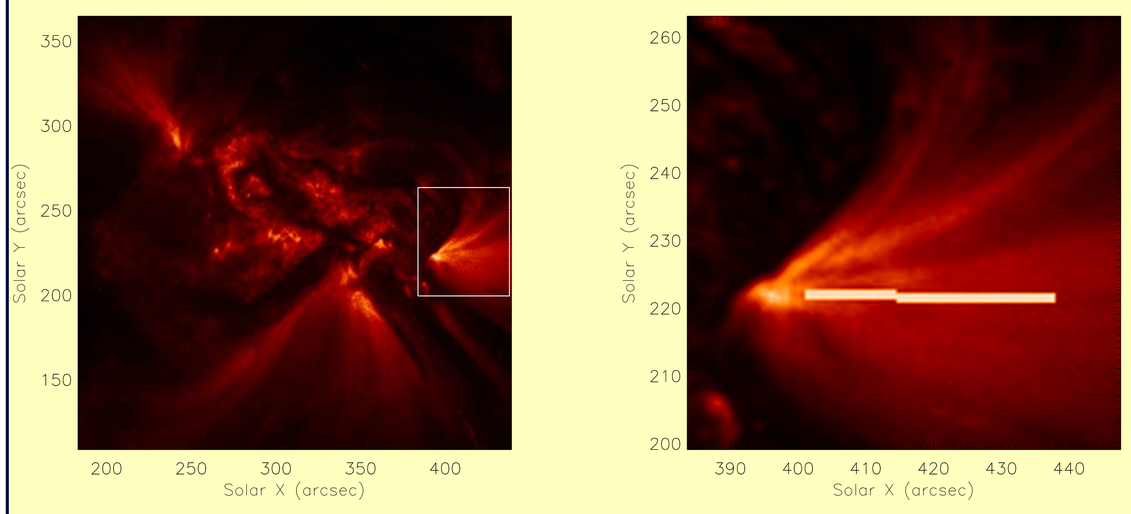

Figure.1 (Left): Active Region 8253 at 171Å banpass imaged by TRACE at 12:00 UT on 30 - Jun - 1998; (Right): The region of interest ($54 \times 64\,\mathrm{arcsec}^2$), The line indicates the positioning of the slit used in the time-distance plot.

The cadence time of the observation was either about 41 s or 30 s for both EUV bandpasses, 195Å images were normally taken about 11 s later than the 171Å ones (Fig.2). The data contained several gaps, but the observations covered about $\sim 70\%$ and $\sim 40\%$ of the time interval in the 171Å and 195Å bandpasses, respectively.

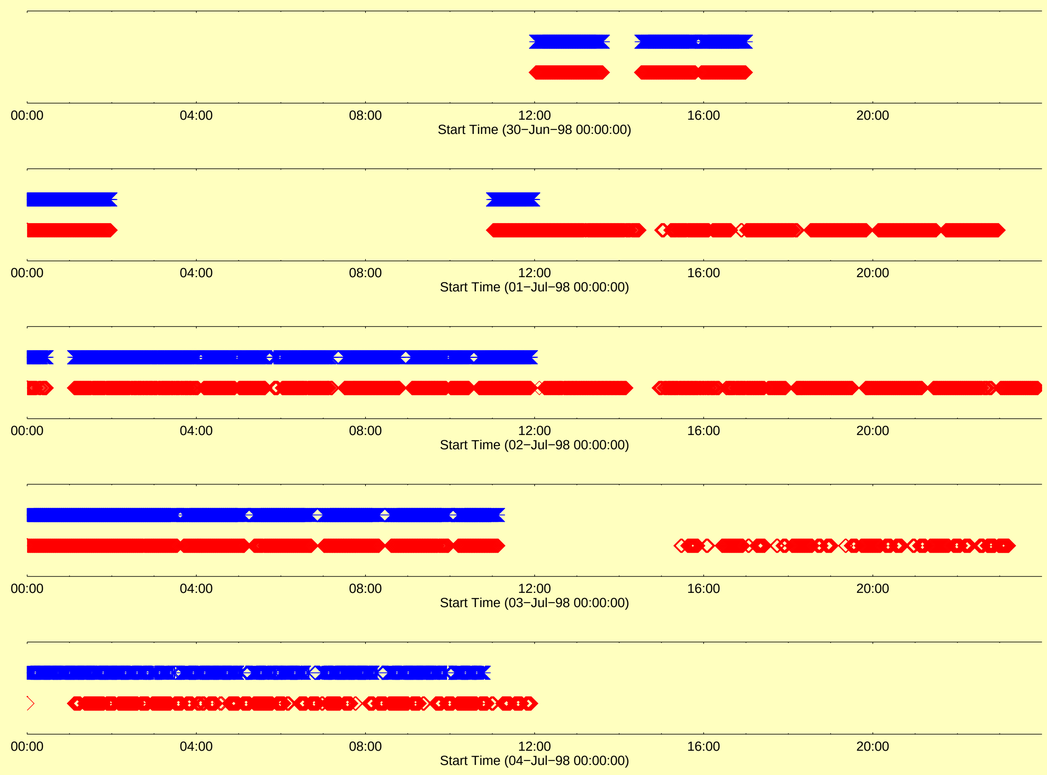

Figure.2. Observational coverage of AR8253 at 171Å(red) and 195Å(blue) by TRACE in the analysed time interval. Small data gaps of order 100 s are due to channel switching, and large ones are due to routine observations on the solar limb (including polar regions), re-pointing or to avoid radiation belts.

Data Preparation

The datacubes are prepared from FITS files by the standard routine TRACE_PREP with standard pre-processing keywords. The EUV images are calibrated with white light pointing; the spikes and streaks from radiation belts and cosmic rays, plus the readout noise, are removed; the flux intensities are normalised to exposure time. The image coordinates are co-aligned at the origin of solar disk in the Heliocentric-Cartesian Coordinates, after co-alignment processing of spacecraft re-targeting, the fan-like structure (Fig.1, left panel) is tracked in the co-moving frame of solar surface rotation. The spacecraft pointing drifts, plus the uncertainties of solar rotational model, are minimised by cross-correlation offsets, the images are smoothed with a box car of 10×10 pixels beforehand, and the cross-correlation offsets are further smoothed to suppress the perturbations caused by small dynamic features. Two corrected sub dataset (108×128 pixels image size in 171Å and 195Å) are taken for further analysis (Fig.1 right panel).

Preliminary Analysis

We analysed the first continuous segment of the time series (Fig.2, starting from 12:00 UT, lasting ~ 100 mins) of a macro pixel (3×3 pixels) located mid-way along the slit (Fig.1)

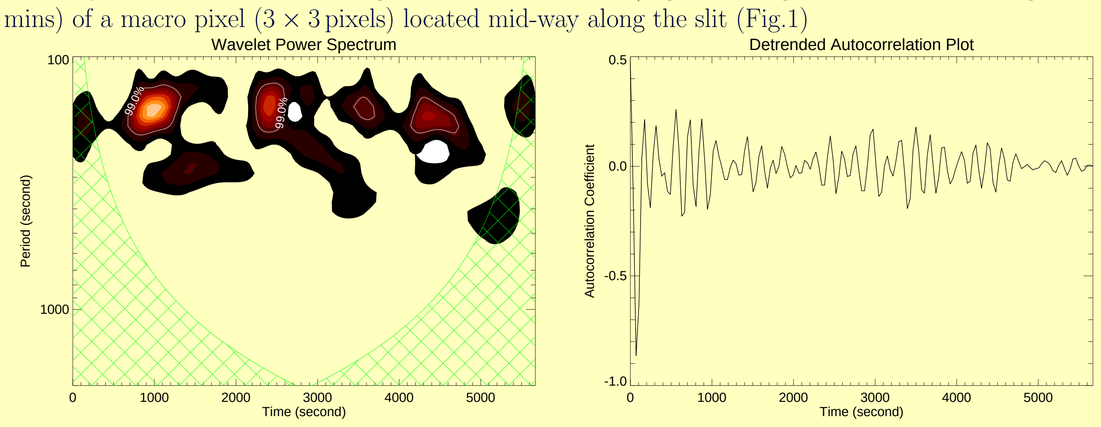

Figure.3 (Left): Wavelet Power Spectrum showing 180 s oscillation trains. The significant levels above 99.0% are contoured round the peak powers. The Cone of Influence (COI) due to zero paddings is cross-hatched; (Right): Autocorrelation plot, good harmonic oscillations with stable phase are found to agree in time with the blobs at wavelet power spectrum.

Running Difference

Our initial analysis is focused on the first 10 cycles of the time series shown in Fig.3, we display the running difference of the intensities along the slit (Fig.1, right) over time.

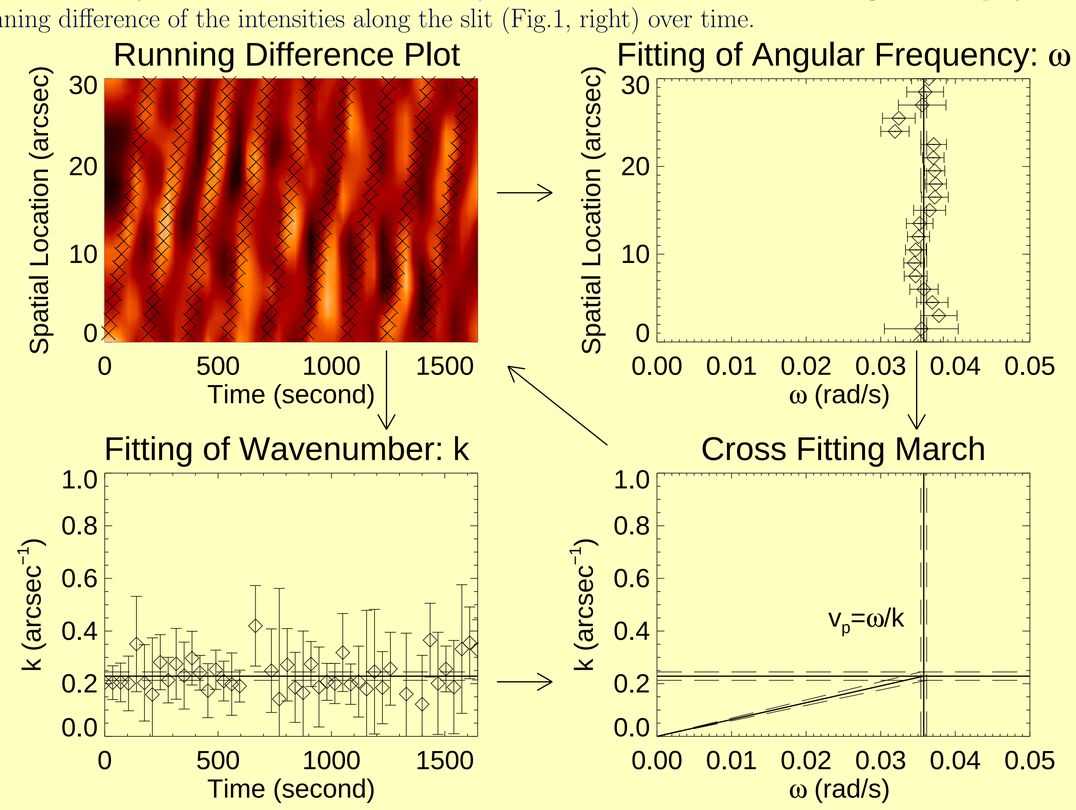

Figure.4. The Cross-Fitting Technique: The running difference plot is assumed to be in form of $A\cos(\omega t - kx + \phi_0)$ for ~ 10 cycles. Both angular frequency and wavenumber are approximated by fitting the intensity variation with cos function (Levenberg-Marquardt least-squares method). The weighted means of both ω and k are calculated and give the apparent phase speed $v_p = \omega/k$. The average best-fitted phase speed is shown by crosses in the running difference plot, demonstrating the good agreement with the visually identified diagonal structures. The parameters of the propagating wave are estimated as: the angular frequency $\omega = 0.0357 \pm 0.0039\,\mathrm{rad/s}$, wavenumber $k = 0.229 \pm 0.016\,\mathrm{arcsec}^{-1}$, the phase speed $v_p = 113 \pm 8\,\mathrm{km/s}$.

Hough Transform

The projected phase speed of the propagating waves, determined by the running difference time-distance plot, is also measured with the Hough Transform method (Ballester 1994).

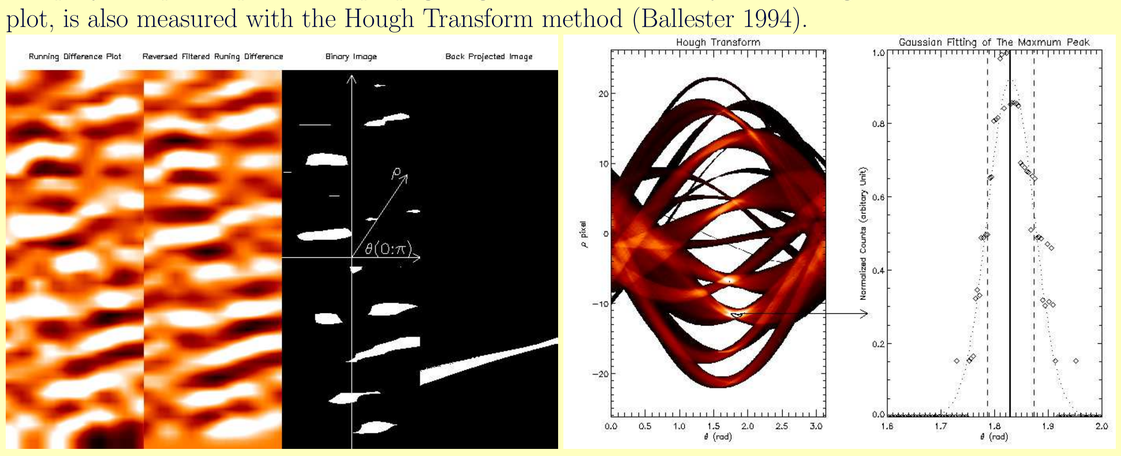

Figure.5 (Left): Steps of Hough Transform method. The running difference plot is convolved with a derivative filter and futher reversed, then it is made into binary image by thresholding at 50% of global maximum. (Right): The Hough Transform plot. The dominant peak is picked by selecting votes above 80% of the peak. Gaussian fitting gives the value of the gradient of the corresponding straight line in the image. The measured ridge correspond to the phase speed $v_p = 117 \pm 20\,\mathrm{km/s}$.

Conclusion

- A robust, fully automatic and accurate method for the measurement of the apparent speed, based upon the Cross-Fitting (Hough transform) technique, is developed.
- The next stage of the project is to study the time-variability of the phase speed and period of the waves

References

1. Ballester, P., 1994. Hough transform for robust regression and automated detection. A&A, **286**, 1011-1018.
2. De Moortel, I., 2006, Propagating magnetohydrodynamics waves in coronal loops, Royal Soc. Lon. Trans. Ser. A, **364**, 461-472.
3. De Moortel, I., 2009. Longitudinal Waves in Coronal Loops. Space Science Reviews, **149** (1-4), 65-81.
4. Nakariakov, V. Verwichte, E., 2005. Coronal Waves and Oscillations. Live Reviews in Solar Physics.